

# Probing ALPs and the Axiverse with Superconducting Radiofrequency Cavities

Zachary Bogorad,<sup>1,\*</sup> Anson Hook,<sup>2,†</sup> Yonatan Kahn,<sup>3,4,‡</sup> and Yotam Soreq<sup>5,6,§</sup>

<sup>1</sup>Laboratory for Nuclear Science, Massachusetts Institute of Technology, Cambridge, MA 02139, U.S.A.

<sup>2</sup>Maryland Center for Fundamental Physics, Department of Physics,  
University of Maryland, College Park, MD 20742, U.S.A.

<sup>3</sup>Kavli Institute for Cosmological Physics, University of Chicago, Chicago, IL 60637, U.S.A.

<sup>4</sup>University of Illinois Urbana-Champaign, Urbana, IL 61801, U.S.A.

<sup>5</sup>Theoretical Physics Department, CERN, CH-1211 Geneva 23, Switzerland

<sup>6</sup>Department of Physics, Technion, Haifa 32000, Israel

(Dated: May 16, 2022)

Axion-like particles (ALPs) with couplings to electromagnetism have long been postulated as extensions to the Standard Model. String theory predicts an “axiverse” of many light axions, some of which may make up the dark matter in the universe and/or solve the strong CP problem. We propose a new experiment using superconducting radiofrequency (SRF) cavities which is sensitive to light ALPs independent of their contribution to the cosmic dark matter density. Off-shell ALPs will source cubic nonlinearities in Maxwell’s equations, such that if a SRF cavity is pumped at frequencies  $\omega_1$  and  $\omega_2$ , in the presence of ALPs there will be power in modes with frequencies  $2\omega_1 \pm \omega_2$ . Our setup is similar in spirit to light-shining-through-walls (LSW) experiments, but because the pump field itself effectively converts the ALP back to photons inside a single cavity, our sensitivity scales differently with the strength of the external fields, allowing for superior reach as compared to experiments like OSQAR while utilizing current technology. Furthermore, a well-defined program of increasing sensitivity has a guaranteed physics result: the first observation of the Euler-Heisenberg term of low-energy QED at energies below the electron mass. We discuss how the ALP contribution may be separated from the QED contribution by a suitable choice of pump modes and cavity geometry, and conclude by describing the ultimate sensitivity of our proposed program of experiments to ALPs.

Axions are well motivated new particles that have been proposed as a solution to the strong CP problem [1–3] (for a review of axions see Refs. [4–6]). Additionally the only known consistent theory of quantum gravity, string theory, predicts a plethora of light ( $\ll$  eV) particles [7], some of which may couple to electromagnetism in a manner very similar to the axion. These particles have been termed axion-like particles (ALP) and the (possibly) large number of ALPs can be called the “axiverse” [8]. One or more of these species may be excellent dark matter (DM) candidates [9–11], and/or alleviate the hierarchy problem [12–16]. In light of this strong motivation, there has been much experimental effort devoted towards looking for the axion and its cousins [17, 18].

There are several general approaches for finding ALPs, roughly analogous to the multipronged approach of direct detection, indirect detection, and collider production for WIMP DM. If the ALP makes up the DM of the Universe, it may be detected in the laboratory by converting ALPs to electromagnetic energy (see Refs. [19–21] for recent experimental results) or rotating the polarization of photons [22, 23], or in radio telescopes by searching for conversion [24–27] or decay [28, 29] to photons in astrophysical environments. Another approach which does not

require the ALP to be DM is colloquially known as light-shining-through-walls (LSW): a laser passes through a large magnetic field, some photons convert to ALPs, a wall blocks the remaining photons but not the ALPs, and after the wall another large magnetic field converts the ALPs back into detectable photons. LSW experiments have the advantage that both ALP production and detection are completely under experimental control. Such experiments are also “broadband” in the sense that they are simultaneously sensitive to a wide range of ALP masses, and indeed multiple species of ALPs.

In this Letter, we propose a new experiment along the lines of an LSW experiment that utilizes light-by-light scattering mediated by *off-shell* ALPs, with production and detection taking place inside the *same* superconducting radiofrequency (SRF) cavity. An ALP  $a$  is a pseudoscalar defined by its mass  $m_a$  and its coupling to electromagnetism  $g_{a\gamma\gamma}$ . Its Lagrangian is

$$\mathcal{L}_a = \frac{1}{2}\partial_\mu a \partial^\mu a - \frac{1}{2}m_a^2 a^2 - \frac{1}{4}g_{a\gamma\gamma} a F_{\mu\nu} \tilde{F}^{\mu\nu}. \quad (1)$$

For processes involving photons with typical energy  $\omega$ , an ALP with mass  $m_a \gg \omega$  may be integrated out, giving an effective Lagrangian [30]

$$\mathcal{L}_{a,\text{eff}} = \frac{g_{a\gamma\gamma}^2}{32m_a^2} (F_{\mu\nu} \tilde{F}^{\mu\nu})^2. \quad (2)$$

In other words, an off-shell ALP will induce small nonlinearities in electromagnetism, by which signal photons may be detected at a different frequency than the input

\*Electronic address: zbogorad@mit.edu

†Electronic address: hook@umd.edu

‡Electronic address: ykahn@uchicago.edu

§Electronic address: yotam.soreq@cern.ch

photons. Note that this effect is *local*, and does not require the ALP to propagate to another spacetime point to be converted back to photons. Of course, we are also interested in ALPs which are very light. As such, we will extend the analysis of [30] to the case where  $m_a \ll \omega$ . In this case the nonlinear effects are nonlocal, but we will show that detection of signal photons may still take place in the same spacetime region as the input photons.

Famously, loop contributions from virtual electrons will also induce such nonlinearities in pure quantum electrodynamics (QED), which are parameterized by the Euler-Heisenberg (EH) Lagrangian [31, 32]. To lowest order in  $\alpha$  and  $\omega/m_e$ , this is

$$\mathcal{L}_{\text{EH}} = \frac{\alpha^2}{360m_e^4} \left[ 4(F_{\mu\nu}F^{\mu\nu})^2 + 7(F_{\mu\nu}\tilde{F}^{\mu\nu})^2 \right], \quad (3)$$

valid for  $\omega \ll m_e$ . Light-by-light scattering with real photons has recently been observed at GeV energies [33], but Eq. (3) has never been probed with real photons at  $\omega < m_e$ . Thus, an experiment that is designed to look for non-linearities induced by ALPs would, if sensitive enough, also have the guaranteed physics result of discovering light-by-light scattering at low energies for the first time ever! Crucially, the effects of ALPs and the EH Lagrangian are not exactly degenerate, as the ALP Lagrangian only contains  $F_{\mu\nu}\tilde{F}^{\mu\nu} \propto \mathbf{E} \cdot \mathbf{B}$ , while the EH Lagrangian also contains  $F_{\mu\nu}F^{\mu\nu} \propto \mathbf{E}^2 - \mathbf{B}^2$ . Thus, the two effects are linearly independent and may be disentangled with a suitable choice of field configurations.

Comparing Eqs. (2)–(3), we expect the ALP contribution to 4-photon processes to exceed the EH contribution when [30, 34]

$$\frac{g_{a\gamma\gamma}}{m_a} \gtrsim \mathcal{O}(1) \times \frac{\alpha}{m_e^2} \simeq \frac{10^{-10} \text{ GeV}^{-1}}{10^{-6} \text{ eV}}. \quad (4)$$

The best laboratory bounds on  $g_{a\gamma\gamma}$  are from the OSQAR [35] and PVLAS [36] experiments, which constrain  $g_{a\gamma\gamma} < 3.5 \times 10^{-8} \text{ GeV}^{-1}$  for  $m_a \lesssim 10^{-4} \text{ eV}$ . Surpassing these bounds with a radiofrequency experiment ( $\omega \sim 10^{-6} \text{ eV}$ ) would not require sensitivity to the EH Lagrangian, since the ALP term in the Lagrangian would be much larger. Under reasonable assumptions about solar physics, the bounds from the CAST experiment [37] constrain  $g_{a\gamma\gamma} < 6.6 \times 10^{-11} \text{ GeV}^{-1}$  from thermal ALPs produced in the sun. (More stringent bounds can be obtained for  $m_a \lesssim 10^{-10} \text{ eV}$  from the absence of photon-ALP oscillations in galactic magnetic fields [38–41].) An experiment which surpasses these bounds would also be sensitive to the EH contribution, as the ALP contribution would be of similar size.

Taking these estimates as motivation, a very interesting proposal [42, 43] suggested a setup for detecting the EH Lagrangian using SRF cavities. In this Letter, we extend the results of Ref. [43] to include the contributions from the ALP Lagrangian (1). Such contributions have been considered before [34], but in the context of

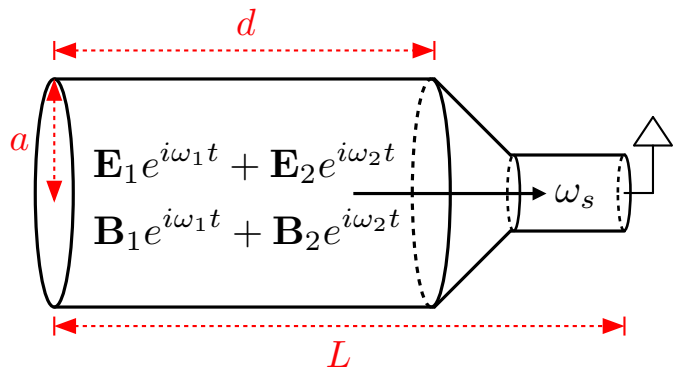


FIG. 1: Schematic of our proposed experiment, adapted from Ref. [43]. An SRF cavity is pumped at frequencies  $\omega_1$  and  $\omega_2$ . The signal mode  $\omega_s$  (equal to  $2\omega_1 - \omega_2$  in our examples), sourced either by ALPs or the EH Lagrangian, is detected in a filtering region and amplified. Note that  $\omega_s$  extends through the bulk of the cavity, but the filtering geometry suppresses the pump fields in the detection region.

colliding laser beams and momentum-space Feynman diagrams, which are not appropriate for the boundary conditions imposed by cavity experiments.

Furthermore, while it was demonstrated in [34] that such contributions will likely never be sensitive to the so-called QCD axion which solves the strong-CP problem [1–3], renewed interest in the axiverse strongly motivates a re-examination of this result for general ALPs. Indeed, multiple ALPs will all contribute to nonlinearities in electromagnetism. In a standard on-shell ALP search, e.g. a LSW experiment, if all the couplings of the ALPs are of the same order  $g_{a\gamma\gamma}$ , the strength of the effect scales as  $\mathcal{N}_a g_{a\gamma\gamma}^4$ , where  $\mathcal{N}_a$  is the number of ALPs lighter than the typical energy scale  $\omega$  of the photons in the experiment (e.g. 2.33 eV for OSQAR). By contrast, because our proposed experiment is sensitive to off-shell ALPs, our signal scales as  $\mathcal{N}_a^2 g_{a\gamma\gamma}^4$ , better than any previous experiment. Sufficiently strong bounds on this product may begin to constrain axiverse scenarios which predict large numbers of light ALPs, for example compactification manifolds with large numbers of non-trivial cycles [44].

*ALP-induced cavity source terms.* Equation (1) implies that Maxwell’s equations are modified in the presence of nonzero  $g_{a\gamma\gamma}$  [45]. Ignoring the EH terms for now, the modified equations of motion for  $\mathcal{N}_a$  ALPs with zero external charges or currents are

$$\nabla \cdot \mathbf{E} = \mathbf{B} \cdot \sum_{i=1}^{\mathcal{N}_a} g_{a\gamma\gamma}^{(i)} \nabla a_i, \quad (5)$$

$$\nabla \times \mathbf{B} = \frac{\partial \mathbf{E}}{\partial t} - \mathbf{E} \times \sum_{i=1}^{\mathcal{N}_a} g_{a\gamma\gamma}^{(i)} \nabla a_i + \mathbf{B} \sum_{i=1}^{\mathcal{N}_a} g_{a\gamma\gamma}^{(i)} \frac{\partial a_i}{\partial t}, \quad (6)$$

$$(\partial_t^2 - \nabla^2 + m_{a_i}^2) a_i = g_{a\gamma\gamma}^{(i)} \mathbf{E} \cdot \mathbf{B} \quad (i = 1, \dots, \mathcal{N}_a). \quad (7)$$

We will assume that the  $g_{a\gamma\gamma}^{(i)}$  are small and use classical field perturbation theory. Equation (7) shows that regions of nonzero  $\mathbf{E} \cdot \mathbf{B}$  in a conducting cavity will source

the  $a_i$  field proportional to  $g_{a\gamma\gamma}^{(i)}$ ; Eqs. (5)–(6) imply that  $a_i$  will in turn source signal fields cubic in the cavity fields and proportional to  $(g_{a\gamma\gamma}^{(i)})^2$ . If all the  $g_{a\gamma\gamma}^{(i)}$  are identical, the signal fields will be proportional to  $\mathcal{N}_a g_{a\gamma\gamma}^2$ .

Unless otherwise specified, we now restrict to the case of a single ALP,  $\mathcal{N}_a = 1$ . We may use the Green's function for the ALP field to write the signal fields solely in terms of the cavity fields, which we refer to as *pump* fields from now on. The appropriate Green's function is the classical retarded Green's function for the Klein-Gordon equation  $G_R(\mathbf{x}, t, \mathbf{x}', t')$ . The solution for  $a(\mathbf{x}, t)$  is then

$$a(\mathbf{x}, t) = g_{a\gamma\gamma} \int d^3\mathbf{x}' dt' G_R(\mathbf{x}, t, \mathbf{x}', t') \mathbf{E}(\mathbf{x}', t') \cdot \mathbf{B}(\mathbf{x}', t'). \quad (8)$$

We will consider a cavity pumped *simultaneously* at resonant frequencies  $\omega_1$  and  $\omega_2$ , with associated modes  $\mathbf{E}_1, \mathbf{B}_1$  and  $\mathbf{E}_2, \mathbf{B}_2$ , shown schematically in Fig. 1. The total input electric field in the cavity is  $\mathbf{E}_p = \mathbf{E}_1 e^{i\omega_1 t} + \mathbf{E}_2 e^{i\omega_2 t}$ , where it is understood that the physical field is the real part of the complex field and that the correct phase relationships exist between  $\mathbf{E}$  and  $\mathbf{B}$ . From now on, we will drop the explicit time dependence of the pump modes.

The terms involving derivatives of  $a$  on the right-hand side of Eqs. (5)–(6) can be interpreted as an effective ALP charge and current:

$$\rho_a = g_{a\gamma\gamma} \mathbf{B}_p \cdot \nabla a; \quad \mathbf{J}_a = g_{a\gamma\gamma} \left( \nabla a \times \mathbf{E}_p + \mathbf{B}_p \frac{\partial a}{\partial t} \right). \quad (9)$$

Note that since  $a$  is quadratic in the pump fields,  $\rho_a$  and  $\mathbf{J}_a$  are cubic in the pump fields, and will thus have frequency components  $\omega_1, \omega_2, 2\omega_1 \pm \omega_2$ , and  $2\omega_2 \pm \omega_1$ . If  $\mathbf{E}_p$  and  $\mathbf{B}_p$  satisfy Maxwell's equations, then  $\rho_a$  and  $\mathbf{J}_a$  satisfy the continuity equation  $\partial\rho_a/\partial t + \nabla \cdot \mathbf{J}_a = 0$ . Thus, using the solution for  $a$  in Eq. (8), we may treat  $\mathbf{J}_a$  as a source for the cavity involving only the pump fields  $\mathbf{E}_p$  and  $\mathbf{B}_p$ , identical in formalism to a real current source involving moving charges.

*Signal strength.* To solve for the signal fields, we will use the general formalism of cavity Green's functions [46]. We assume that a signal mode  $\omega_s$  is a resonant mode of the cavity which matches one of the frequency components of  $\mathbf{J}_a$ . Assuming a finite quality factor  $Q_s$  for this mode, the ALP-sourced  $\mathbf{E}_a$  field which develops in a cavity of volume  $V$  is

$$\mathbf{E}_a(\mathbf{x}) = \frac{Q_s}{\omega_s V} \hat{\mathbf{E}}_s(\mathbf{x}) \int d^3\mathbf{x}' \hat{\mathbf{E}}_s(\mathbf{x}') \cdot \mathbf{J}_a(\mathbf{x}'), \quad (10)$$

where  $\hat{\mathbf{E}}_s$  is dimensionless with normalization  $\int d^3\mathbf{x} |\hat{\mathbf{E}}_s(\mathbf{x})|^2 = V$ .

To estimate the size of the signal, we normalize the pump modes such that  $\int d^3\mathbf{x} |\mathbf{E}_1(\mathbf{x})|^2 = \int d^3\mathbf{x} |\mathbf{E}_2(\mathbf{x})|^2 = E_0^2 V$ , and write  $\mathbf{J}_a = \kappa_{m_a} E_0^3 \hat{\mathbf{J}}_a$  where  $\hat{\mathbf{J}}_a$  is dimensionless and  $\kappa_{m_a}$  has dimension  $-3$ . In the two limiting cases of  $m_a \gg \omega_s$  and  $m_a \ll \omega_s$ , we choose

$\kappa_{m_a}$  to be  $\kappa_\infty = g_{a\gamma\gamma}^2 \omega_s / m_a^2$  and  $\kappa_0 = g_{a\gamma\gamma}^2 / \omega_s$ , respectively. The number of photons in the signal field is

$$N_s = \frac{1}{2\omega_s} \int d^3\mathbf{x} |\mathbf{E}_a(\mathbf{x})|^2 = \frac{Q_s^2 V E_0^6}{2\omega_s^3} \kappa_{m_a}^2 K_{m_a}^2, \quad (11)$$

where we have defined the dimensionless cavity form factor

$$K_{m_a} \equiv \frac{1}{V} \left| \int d^3\mathbf{x}' \hat{\mathbf{E}}_s(\mathbf{x}') \cdot \hat{\mathbf{J}}_a(\mathbf{x}') \right|. \quad (12)$$

We make explicit the fact that  $K$  and  $\kappa$  both depend on  $m_a$  through the Green's function  $G_R$ , which affects the solution for  $a$  in Eq. (8).

At this point, we do a brief comparison between the parametrics of a LSW experiment and our own proposal. In the low- $m_a$  limit, the number of signal photons per number of input photons,  $N_i$ , in the two experiments scales like

$$\frac{N_s}{N_i} \Big|_{\text{LSW}} \sim g_{a\gamma\gamma}^4 B_{\text{prod.}}^2 B_{\text{det.}}^2 L^4, \quad \frac{N_s}{N_i} \Big|_{\text{cavity}} \sim Q_s^2 g_{a\gamma\gamma}^4 E_0^4 L^4, \quad (13)$$

where  $B_{\text{prod.}}$  and  $B_{\text{det.}}$  refer to the two  $B$ -fields used for production and detection of ALPs, respectively, and  $L$  is the typical size of the experiment (for our setup, we assume  $L \sim 1/\omega_s$ ). Our experiment scales similarly to a LSW experiment except that our final number of photons has been enhanced by  $Q_s^2$  due to the cavity, and there is only a single field region rather than separate production and detection regions; instead of  $B_{\text{prod.}}$  and  $B_{\text{det.}}$ , the input oscillating field  $E_0$  does the conversion. A static  $B$  field can be made about 40 times larger than an oscillating  $B$  field, but this deficit is more than made up for by the large  $Q$  factor of SRF cavities, which can reach  $10^{12}$  [47, 48].

It is worth noting that the scaling of a LSW experiment that utilizes cavities, e.g. ALPS-II, would also be enhanced by  $Q$ , but such cavities could not be made superconducting at  $B$ -fields above a few T, and the largest  $Q$  achievable in copper cavities is about  $10^6$ . Our cavity experiment would still have superior sensitivity to such an LSW experiment, unless the ALP were both produced and detected in high- $Q$  SRF cavities, where the larger  $Q$  compensates for the smaller  $B$  [49, 50]. Furthermore, in our setup, the detection frequency is not a harmonic of the input frequency, which may help reduce backgrounds. In the large mass limit of a LSW experiment,  $N_s/N_i \sim 1/m_a^8$ , until  $\omega \sim m_a$  and then ALP photon conversions cannot occur. In the large mass limit of our proposal,  $N_s/N_i \sim 1/m_a^4$ , giving a much better reach at large masses.

*Cavity form factors: heavy and light ALPs.* To understand the signal strength as a function of  $m_a$ , we compute the cavity form factors in two limits:  $K_\infty$ , where  $m_a \gg \omega_s$ , and  $K_0$ , where  $m_a \ll \omega_s$ .

The first case corresponds to ‘‘integrating out’’ the ALP in the context of field theory. By assumption,

$\partial_t^2 a, \nabla^2 a \ll m_a^2 a$  for a heavy ALP, so we can solve algebraically for  $a$  in terms of the pump fields. In this limit, the ALP-induced current is

$$\mathbf{J}_\infty = \frac{g_{a\gamma\gamma}^2}{m_a^2} \left( \nabla(\mathbf{E}_p \cdot \mathbf{B}_p) \times \mathbf{E}_p + \mathbf{B}_p \frac{\partial}{\partial t} (\mathbf{E}_p \cdot \mathbf{B}_p) \right). \quad (14)$$

For the case  $m_a \rightarrow 0$ , the ALP Green's function is identical to the retarded Green's function familiar from electromagnetism:

$$a_0(\mathbf{x}, t) = \frac{g_{a\gamma\gamma}}{4\pi} \int \frac{d^3 \mathbf{x}'}{|\mathbf{x} - \mathbf{x}'|} \mathbf{E}_p(\mathbf{x}', t_R) \cdot \mathbf{B}_p(\mathbf{x}', t_R), \quad (15)$$

where  $t_R = t - |\mathbf{x} - \mathbf{x}'|$  is the retarded time. In this case,  $a$  responds nonlocally to changes in  $\mathbf{E}_p$  and  $\mathbf{B}_p$ , with a time delay given by  $t_R$ . Since the ALP-mediated current  $\mathbf{J}_0$ , which may be computed from Eq. (15) using Eq. (9), is also nonlocal, there is no simple expression in terms of the pump fields.

As an example, we calculate the cavity form factor for a right cylindrical cavity with the mode choices  $\omega_1 = \text{TE}_{011}$  and  $\omega_2 = \text{TM}_{010}$  (with mode labeling conventions following [46]). We choose the signal mode  $\omega_s = 2\omega_1 - \omega_2$  to be  $\text{TM}_{020}$ , which is satisfied for a cavity of radius  $a$  and height  $d = 3.112a$ . For this mode combination, we find  $K_\infty = 0.18$  for the heavy ALP and  $K_0 = 0.24$  for the light ALP (see Supplementary Material for details). The latter result assumes that both  $\sin(\omega_s t)$  and  $\cos(\omega_s t)$  components of the signal can be added in quadrature, which is appropriate for photon counting at the standard quantum limit.

This example demonstrates that there exist modes for which the cavity form factor is relatively insensitive to  $m_a$ , and thus a single cavity can be used to probe a broad range of ALP masses. This is one of the strongest advantages of our setup over traditional resonant searches for ALP dark matter [19, 20, 51, 52], which require careful tuning to match a resonance (e.g. a cavity mode or a Larmor frequency) to  $m_a$ . By contrast, once the tuning  $\omega_s = 2\omega_1 - \omega_2$  is accomplished, no further tuning is required to set limits on  $g_{a\gamma\gamma}$  for any  $m_a$ .

*Expected sensitivity to ALPs.* In order to estimate the sensitivities in the light and heavy mass limits, we compute the expected number of photons  $N_s$ . From Eq. (11) we have

$$N_{s,0} = \frac{Q_s^2 V E_0^6}{2\omega_s} \frac{g_{a\gamma\gamma}^4}{\omega_s^4} K_0^2, \quad N_{s,\infty} = \frac{Q_s^2 V E_0^6}{2\omega_s} \frac{g_{a\gamma\gamma}^4}{m_a^4} K_\infty^2. \quad (16)$$

To measure the signal, we imagine a filtering geometry as suggested in Ref. [43] (and shown in Fig. 1) where at some point in the geometry the pump fields are suppressed compared to the signal field, which is possible as long as  $\omega_s > \omega_{1,2}$ . At this location, the signal can be measured without contamination from the pump modes. Because we know the input fields and their phases, we can calculate the waveform of the signal as a function of time. We naively estimate the signal-to-noise ratio (SNR) by

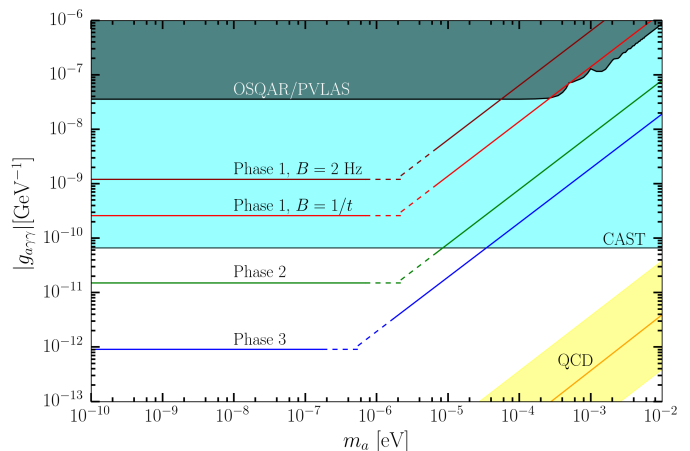


FIG. 2: Projected sensitivities of our proposed Phases 1, 2, and 3 (approximations for  $m_a \sim \omega_s$  shown in dashed lines), along with existing constraints from OSQAR [35], PVLAS [36], and CAST [37], and the parameter space for the QCD axion. In particular, Phase 2 could simultaneously set world-leading limits on  $g_{a\gamma\gamma}$  while also measuring the EH contribution to light-by-light scattering below the electron mass for the first time.

using the Dicke radiometer equation and neglecting any information about the field phase:

$$\text{SNR} = \frac{P_s}{T} \sqrt{\frac{t}{B}} \approx \frac{N_s}{N_{\text{th}}} \frac{1}{2LQ_s} \sqrt{\frac{t}{B}}, \quad (17)$$

where  $P_s$  is the signal power,  $t$  is the total measurement time,  $B$  is the signal bandwidth,  $L$  is the length of the cavity, and  $N_{\text{th}} = T/\omega_s$  is the number of thermal photons at the signal frequency (valid for temperatures  $T \gg \omega_s$ , and assuming thermal noise dominates). A detailed sensitivity calculation exploiting phase-sensitive amplifiers will be presented in a future work.

Our expected sensitivity to  $g_{a\gamma\gamma}$  is then

$$g_{a\gamma\gamma}^{\text{lim.}} = \begin{cases} \left( \frac{4TL}{Q_s V E_0^6} \sqrt{\frac{B}{t}} \text{SNR} \right)^{1/4} K_0^{-1/2} \omega_s, & m_a \ll \omega_s \\ \left( \frac{4TL}{Q_s V E_0^6} \sqrt{\frac{B}{t}} \text{SNR} \right)^{1/4} K_\infty^{-1/2} m_a, & m_a \gg \omega_s. \end{cases} \quad (18)$$

In an actual experimental implementation, a cavity should be designed specifically to maximize the figure of merit in Eq. (18) while minimizing issues such as multipacting, dark currents, field emission, and surface nonlinearities [53, 54].

For a fixed choice of modes and cavity size (and hence fixed  $\omega_s$  and  $V$ ), the reach is constant at small  $m_a$  and degrades linearly at large  $m_a$ . There is in principle some dependence of  $K_{m_a}$  on  $m_a$ , but as our example above demonstrates, with a suitable choice of modes this dependence is extremely mild. For a large number  $\mathcal{N}_a$  of light ALPs, all with  $m_a \ll \omega_s$ , the limit in Eq. (18)

should be interpreted as a limit on  $\sqrt{\sum_{i=1}^{\mathcal{N}_a} (g_{a\gamma\gamma}^{(i)})^2}$ .

*Phase 1: Conservative projected reach.* We envision our experiment progressing in three stages, each build-

ing on current technology. For Phase 1, we take the following parameters: cavity temperature  $T = 1.5$  K; a right cylindrical cavity of radius  $a = 0.5$  m and the  $\text{TE}_{011}/\text{TM}_{010}/\text{TM}_{020}$  mode combination giving height  $d = 1.56$  m and  $f_s = \omega_s/(2\pi) = 527$  MHz; cavity volume  $V = 1.23$  m<sup>3</sup>;  $K_0 = 0.4$  as calculated above; pump field strength  $E_0 = 45$  MV/m; and a cavity bandwidth of  $f_s/Q_s = 2$  Hz, corresponding to  $Q_s = 2.6 \times 10^8$ . This  $Q$  is much smaller than what typical high-performance SRF cavities can achieve, but a wide cavity response function for Phase 1 allows the frequency-matching condition  $\omega_s = 2\omega_1 - \omega_2$  to be approximately satisfied even if vibrational distortions of the cavity geometry shift  $\omega_s$  by  $\mathcal{O}(\text{Hz})$ . Note also that our mode combination satisfies  $\omega_s > \omega_1, \omega_2$ , making it amenable to filtering; to model this, we assume the total cavity length is twice the cavity height,  $L = 3.12$  m.

At 1.5 K, the thermal noise in the signal mode is  $N_{\text{th}} = kT/\omega_s \simeq 60$  photons. A lower operating temperature would be desirable, but the cooling power requirements are substantial: assuming that the pump modes have  $Q_{1,2} = 10^{12}$ , characteristic of the best  $Q$  achieved in SRF cavities [47, 48], the cavity lifetime for the pump modes is  $\tau_{1,2} = Q_{1,2}/f_{1,2} \sim 2600$  s and the power dissipated is  $\mathcal{O}(10$  W). Since dilution refrigerators have a cooling capacity of  $\mathcal{O}(\text{mW})$ , the cavity must be operated at liquid helium temperatures.

We first consider the case where the injected pump bandwidth is comparable to the cavity bandwidth,  $B = 2$  Hz. For light ALPs a SNR of 5 can be achieved at  $g_{a\gamma\gamma} = 5.3 \times 10^{-9}$  GeV, surpassing the OSQAR bound by nearly an order of magnitude in a single cavity lifetime of  $\tau_s = Q_s/f_s = 0.5$  s. Integrating the signal over a time  $t \sim 1$  day, we can obtain a Phase 1 reach of  $g_{a\gamma\gamma,0}^{\text{lim.}} = 1.2 \times 10^{-9}$  GeV<sup>-1</sup>. For  $m_a \gg \omega_s$ , we can get the limits by using  $g_{a\gamma\gamma,\infty}^{\text{lim.}} = (m_a/\omega_s)\sqrt{K_0/K_\infty} g_{a\gamma\gamma,0}^{\text{lim.}}$ .

One could also pump the cavity with a bandwidth narrower than the cavity itself, for example by locking the pump tones to an atomic clock. Taking  $B = 1/t$ , the narrowest allowed bandwidth for a given measurement time  $t$ , a bound of  $g_{a\gamma\gamma,0}^{\text{lim.}} = 2.6 \times 10^{-10}$  GeV<sup>-1</sup> could be reached in a day. In the case  $B = 1/t$ , the signal to noise scales linearly with time, so the limit on  $g_{a\gamma\gamma}$  scales as  $t^{1/4}$ . The two bandwidth choices for Phase 1 are shown in Fig. 2; we have not explicitly calculated the reach for  $m_a \sim \omega_s$  (shown as dashed lines), but we expect the light and heavy mass limits to be excellent approximations away from this region.

*Phase 2: Detecting the Euler-Heisenberg contribution.* As we have discussed, there is an irreducible contribution to cubic nonlinearities in Maxwell's equations from the EH Lagrangian, see Eq. (3). The effective EH charge and current are [42, 55]

$$\rho_{\text{EH}} = -\frac{4\alpha^2}{45m_e^4} \nabla \cdot \mathbf{P}; \quad \mathbf{J}_{\text{EH}} = \frac{4\alpha^2}{45m_e^4} \left( \nabla \times \mathbf{M} + \frac{\partial \mathbf{P}}{\partial t} \right), \quad (19)$$

with  $\mathbf{P} = 7(\mathbf{E} \cdot \mathbf{B})\mathbf{B} + 2(\mathbf{E}^2 - \mathbf{B}^2)\mathbf{E}$  and  $\mathbf{M} = 7(\mathbf{E} \cdot \mathbf{B})\mathbf{E} -$

$2(\mathbf{E}^2 - \mathbf{B}^2)\mathbf{B}$ . The number of photons from the EH signal can be estimated similarly to the ALP case.

For Phase 2, we assume the cylindrical cavity geometry from Phase 1, but with  $Q_s = 10^{12}$ . Indeed, in tuned SQUID magnetometers, a feedback circuit may be used to broaden the bandwidth without sacrificing  $Q$  [56]; such a scheme may be possible here. We find that

$$N_{\text{EH}} = \frac{Q_s^2 V E_0^6}{2\omega_s^3} \kappa_{\text{EH}}^2 K_{\text{EH}}^2 \approx 3.6 \quad (20)$$

with  $\kappa_{\text{EH}} = 4\alpha^2 \omega_s / (45m_e^4)$  and  $K_{\text{EH}} = \frac{1}{V} \int d^3\mathbf{x}' \hat{\mathbf{J}}_{\text{EH}} \cdot \hat{\mathbf{E}}_s = 0.18$ , with  $\hat{\mathbf{J}}_{\text{EH}}$  defined analogously to  $\hat{\mathbf{J}}_a$ . This signal strength is roughly consistent with Ref. [43] given our different choices of parameters and modes. Therefore, assuming  $B = 1/t$ , the EH signal can be detected within 20 days of running. The corresponding sensitivity to light ALPs for the same integration time is  $g_{a\gamma\gamma,0}^{\text{lim.}} = 1.6 \times 10^{-11}$  GeV<sup>-1</sup>; this is shown in Fig. 2. This would surpass the CAST bound of  $g_{a\gamma\gamma} = 6.6 \times 10^{-11}$  GeV<sup>-1</sup> and would also be competitive with recent proposals to search for ALP DM at low masses such as ABRACADABRA [21, 57].

If a positive signal were detected, the ALP nature of the signal could be verified with a second cavity with different mode combinations and checking if the size of the second signal matches the expectation from Eq. (16). If the ALP is heavier than  $\omega_s$ , the combination of the two measurements would suffice to determine both  $g_{a\gamma\gamma}$  and  $m_a$ .

Naively, the sensitivity of this proposal to probe ALPs becomes limited when  $N_{\text{EH}} \sim N_s$  and the EH signal becomes an irreducible background. In principle, one can search for the ALP signal on the top of the thermal and EH backgrounds, but as with the ‘‘neutrino floor’’ in WIMP direct detection experiments, the SNR will grow much slower than  $t^{1/4}$ . However, using a suitable choice of modes with a slightly different cavity design, the EH contribution can be removed, leaving behind only the ALP signal. The idea is to pump an additional mode degenerate with  $\omega_1$  but with a different field configuration. By tuning the three different pump amplitudes, we can arrange to have  $K_{\text{EH}} = 0$  with  $K_{m_a} \neq 0$ . For these special pump amplitudes, the EH contribution to light-by-light scattering vanishes at *amplitude* level, and there is no interference with the ALP amplitude.

We demonstrate the idea by considering a rectangular cavity of dimensions  $a \times b \times c$  and the limit of  $m_a \gg \omega_s$ . The three pump modes (labeled 1, 1', and 2) are  $\text{TE}_{221}/\text{TM}_{221}/\text{TM}_{121}$  and the signal mode is  $\text{TM}_{163}$ . The matching condition  $\omega_s = 2\omega_1 - \omega_2$  is satisfied for  $b = 4a$  and  $c = 1.22a$ . The total pump field is  $\mathbf{E}_p = r_1 \mathbf{E}_1 + r_{1'} \mathbf{E}_{1'} + r_2 \mathbf{E}_2$  (where  $r_1, r_{1'}$ , and  $r_2$  are dimensionless) and similarly for  $\mathbf{B}_p$ . We find

$$\begin{aligned} K_\infty &= 0.047 r_2 (r_1^2 - 0.18 r_{1'}^2), \\ K_{\text{EH}} &= 0.059 r_2 (r_1^2 - 8.24 r_{1'}^2). \end{aligned} \quad (21)$$

Therefore, for  $r_{1'} = 0.35r_1$  we get  $K_{\text{EH}} = 0$  and  $K_\infty = 0.046r_1^2r_2$ .

In the above example, we chose a rectangular cavity for simplicity because TE and TM modes with the same mode numbers are automatically degenerate, and because there is an additional free parameter in the cavity geometry which permits the correct configuration of form factors. We note that this idea can also be implemented with an elliptical cavity, which avoids the large field gradients present at the corners of rectangular cavities, and which may also be used for the Phase 1 search described above.

*Phase 3: Probing the axiverse.* As the optimistic endpoint of this proposed program of experiments, consider a large cylindrical cavity with  $Q_s = 10^{12}$ , radius  $a = 2$  m, and height  $d = 6.22$  m, giving  $f_s = 132$  MHz, with the same mode combinations as considered in Phases 1 and 2. We suppose a cavity geometry can be developed which permits  $K_0 \sim 0.24$  with the EH contribution tuned away to sufficient precision as described in Phase 2, and a compact filtering geometry with length  $L = 10$  m. Using the sensitivity scaling in Eq. (18), assuming the same maximal pump strength of 45 MV/m and integrating for a total time  $t = 1$  year with  $B = 1/t$ , we find a maximum sensitivity at low masses of  $g_{a\gamma\gamma,0}^{\text{lim}} \sim 9.1 \times 10^{-13} \text{ GeV}^{-1}$ , shown in Fig. 2.

Revisiting the axiverse scenario, suppose that  $\mathcal{N}_a$  ALPs all had decay constants  $f_a$  at the string scale, which we conservatively take to be as large as possible, namely the renormalized Planck scale of  $10^{18} \text{ GeV}/\sqrt{\mathcal{N}_a}$ . These string ALPs would have photon couplings of  $g_{a\gamma\gamma} = \alpha/f_a \sim \sqrt{\mathcal{N}_a} 10^{-20} \text{ GeV}^{-1}$ , and our experiment would be

sensitive to  $g_{a\gamma\gamma}\sqrt{\mathcal{N}_a} \sim 10^{-20} \text{ GeV}^{-1} \times \mathcal{N}_a$ . The Phase 3 setup would be able to bound the number of string-scale ALPs with masses less than  $10^{-6} \text{ eV}$  by  $\mathcal{N}_a \lesssim 10^8$ . While this is still (much) larger than typical expectations from string theory, one could still imagine placing constraints on particular compactification geometries which contain large numbers of nontrivial cycles, allowing low-energy SRF cavity experiments to offer a fascinating probe into the ultra-high-energy regime of quantum gravity and the landscape of string theory vacua.

*Acknowledgments.* — AH, YK, and YS thank Ben Safdi and the University of Michigan Slack channel for facilitating discussion in the early stages of this work. YK thanks Prateek Agrawal, M.C. David Marsh, and the participants of the workshop “Axions in Stockholm – Reloaded” for discussions about the axiverse, and James Halverson for discussions about axions in string compactifications. We thank Daniel Bowering, Aaron Chou, Anna Grassellino, Roni Harnik, Kent Irwin, Jonathan Ouellet, Sam Posen, Alexander Romanenko, and Slava Yakovlev for enlightening discussions regarding cavity design and photon readout. We thank Junwu Huang, Gilad Perez and Jesse Thaler for helpful comments on the draft, and Lindley Winslow for support in the early stages of this project. AH is supported in part by the NSF under Grant No. PHY-1620074 and by the Maryland Center for Fundamental Physics (MCFP). The work of ZB is supported by the National Science Foundation under grant number NSF PHY-1806440. This work was supported in part by the Kavli Institute for Cosmological Physics at the University of Chicago through an endowment from the Kavli Foundation and its founder Fred Kavli.

- 
- [1] R. D. Peccei and H. R. Quinn, Phys. Rev. Lett. **38**, 1440 (1977).
- [2] S. Weinberg, Phys. Rev. Lett. **40**, 223 (1978).
- [3] F. Wilczek, Phys. Rev. Lett. **40**, 279 (1978).
- [4] P. Sikivie, Lect. Notes Phys. **741**, 19 (2008), [19(2006)], astro-ph/0610440.
- [5] J. E. Kim and G. Carosi, Rev. Mod. Phys. **82**, 557 (2010), 0807.3125.
- [6] A. Hook (2018), 1812.02669.
- [7] P. Svrcek and E. Witten, JHEP **06**, 051 (2006), hep-th/0605206.
- [8] A. Arvanitaki, S. Dimopoulos, S. Dubovsky, N. Kaloper, and J. March-Russell, Phys. Rev. **D81**, 123530 (2010), 0905.4720.
- [9] J. Preskill, M. B. Wise, and F. Wilczek, Phys. Lett. **B120**, 127 (1983), [URL(1982)].
- [10] L. F. Abbott and P. Sikivie, Phys. Lett. **B120**, 133 (1983), [URL(1982)].
- [11] M. Dine and W. Fischler, Phys. Lett. **B120**, 137 (1983), [URL(1982)].
- [12] P. W. Graham, D. E. Kaplan, and S. Rajendran, Phys. Rev. Lett. **115**, 221801 (2015), 1504.07551.
- [13] R. S. Gupta, Z. Komargodski, G. Perez, and L. Ubaldi, JHEP **02**, 166 (2016), 1509.00047.
- [14] A. Hook and G. Marques-Tavares, JHEP **12**, 101 (2016), 1607.01786.
- [15] O. Davidi, R. S. Gupta, G. Perez, D. Redigolo, and A. Shalit, JHEP **08**, 153 (2018), 1806.08791.
- [16] A. Banerjee, H. Kim, and G. Perez (2018), 1810.01889.
- [17] P. W. Graham, I. G. Irastorza, S. K. Lamoreaux, A. Lindner, and K. A. van Bibber, Ann. Rev. Nucl. Part. Sci. **65**, 485 (2015), 1602.00039.
- [18] I. G. Irastorza and J. Redondo, Prog. Part. Nucl. Phys. **102**, 89 (2018), 1801.08127.
- [19] L. Zhong et al. (HAYSTAC), Phys. Rev. **D97**, 092001 (2018), 1803.03690.
- [20] N. Du et al. (ADMX), Phys. Rev. Lett. **120**, 151301 (2018), 1804.05750.
- [21] J. L. Ouellet et al. (2018), 1810.12257.
- [22] W. DeRocco and A. Hook, Phys. Rev. **D98**, 035021 (2018), 1802.07273.
- [23] H. Liu, B. D. Elwood, M. Evans, and J. Thaler (2018), 1809.01656.
- [24] M. S. Pshirkov, J. Exp. Theor. Phys. **108**, 384 (2009), 0711.1264.
- [25] A. Hook, Y. Kahn, B. R. Safdi, and Z. Sun, Phys. Rev. Lett. **121**, 241102 (2018), 1804.03145.
- [26] F. P. Huang, K. Kadota, T. Sekiguchi, and H. Tashiro,

- Phys. Rev. **D97**, 123001 (2018), 1803.08230.
- [27] B. R. Safdi, Z. Sun, and A. Y. Chen (2018), 1811.01020.
- [28] A. Caputo, C. P. Garay, and S. J. Witte, Phys. Rev. **D98**, 083024 (2018), 1805.08780.
- [29] A. Caputo, M. Regis, M. Taoso, and S. J. Witte (2018), 1811.08436.
- [30] S. Evans and J. Rafelski (2018), 1810.06717.
- [31] W. Heisenberg and H. Euler, Z. Phys. **98**, 714 (1936), physics/0605038.
- [32] J. S. Schwinger, Phys. Rev. **82**, 664 (1951), [,116(1951)].
- [33] M. Aaboud et al. (ATLAS), Nature Phys. **13**, 852 (2017), 1702.01625.
- [34] D. Bernard, Nuovo Cim. **A110**, 1339 (1997), [,201(1997)].
- [35] R. Ballou et al. (OSQAR), Phys. Rev. **D92**, 092002 (2015), 1506.08082.
- [36] F. Della Valle, A. Ejlli, U. Gastaldi, G. Messineo, E. Milotti, R. Pengo, G. Ruoso, and G. Zavattini, Eur. Phys. J. **C76**, 24 (2016), 1510.08052.
- [37] V. Anastassopoulos et al. (CAST), Nature Phys. **13**, 584 (2017), 1705.02290.
- [38] J. W. Brockway, E. D. Carlson, and G. G. Raffelt, Phys. Lett. **B383**, 439 (1996), astro-ph/9605197.
- [39] J. A. Grifols, E. Masso, and R. Toldra, Phys. Rev. Lett. **77**, 2372 (1996), astro-ph/9606028.
- [40] A. Payez, C. Evoli, T. Fischer, M. Giannotti, A. Mirizzi, and A. Ringwald, JCAP **1502**, 006 (2015), 1410.3747.
- [41] M. C. D. Marsh, H. R. Russell, A. C. Fabian, B. P. McNamara, P. Nulsen, and C. S. Reynolds, JCAP **1712**, 036 (2017), 1703.07354.
- [42] G. Brodin, M. Marklund, and L. Stenflo, Phys. Rev. Lett. **87**, 171801 (2001).
- [43] D. Eriksson, G. Brodin, M. Marklund, and L. Stenflo, Phys. Rev. **A70**, 013808 (2004), physics/0411054.
- [44] M. R. Douglas and S. Kachru, Rev. Mod. Phys. **79**, 733 (2007), hep-th/0610102.
- [45] P. Sikivie, Phys. Rev. Lett. **51**, 1415 (1983), [Erratum: Phys. Rev. Lett.52,695(1984)].
- [46] D. Hill, *Electromagnetic Fields in Cavities: Deterministic and Statistical Theories*, IEEE Press Series on Electromagnetic Wave Theory (Wiley, 2009), ISBN 9780470495049.
- [47] A. Romanenko, A. Grassellino, A. C. Crawford, D. A. Sergatskov, and O. Melnychuk, Applied Physics Letters **105**, 234103 (2014), <https://doi.org/10.1063/1.4903808>, URL <https://doi.org/10.1063/1.4903808>.
- [48] A. Romanenko, R. Pilipenko, S. Zorzetti, D. Frolov, M. Awida, S. Posen, and A. Grassellino (2018), 1810.03703.
- [49] R. Harnik, *SRF-based dark matter search: Theory Motivation*, URL <https://indico.fnal.gov/event/19433/session/2/contribution/1/material/slides/0.pdf>.
- [50] A. Grassellino, *SRF-based dark matter search: Experiment*, URL <https://indico.fnal.gov/event/19433/session/2/contribution/2/material/slides/0.pdf>.
- [51] P. Sikivie, N. Sullivan, and D. B. Tanner, Phys. Rev. Lett. **112**, 131301 (2014), 1310.8545.
- [52] D. F. Jackson Kimball et al. (2017), 1711.08999.
- [53] H. Padamsee, Superconductor science and technology **14**, R28 (2001).
- [54] H. Padamsee, *RF superconductivity: science, technology, and applications* (John Wiley & Sons, 2009).
- [55] M. Soljatic and M. Segev, Phys. Rev. **A62**, 043817 (2000).
- [56] W. Myers, D. Slichter, M. Hatridge, S. Busch, M. Mölle, R. McDermott, A. Trabesinger, and J. Clarke, Journal of Magnetic Resonance **186**, 182 (2007).
- [57] Y. Kahn, B. R. Safdi, and J. Thaler, Phys. Rev. Lett. **117**, 141801 (2016), 1602.01086.

# Probing ALPs and the Axiverse with Superconducting Radiofrequency Cavities

## Supplementary Material

Zachary Bogorad, Anson Hook, Yonatan Kahn, Yotam Soreq

In this Supplementary Material, we give further details about the example mode choices we have used to calculate the cavity form factors, and discuss the choice of modes for optimizing our reach for both light and heavy ALPs.

### Mode functions and signal currents

Here we explicitly calculate the axion current and overlap for the mode choices  $\omega_1 = \text{TE}_{011}$ ,  $\omega_2 = \text{TM}_{010}$ , and  $\omega_s = 2\omega_1 - \omega_2 = \text{TM}_{020}$  in a cylindrical cavity of height  $d$  and radius  $a$ , using mode conventions from Ref. [46]. The (un-normalized)  $E$ -field of the signal mode only has a  $z$ -component:

$$\mathbf{E}_s = E_0 J_0 \left( \frac{x_{02} \rho}{a} \right) \hat{\mathbf{z}}, \quad (\text{S1})$$

where  $J_0$  is the Bessel function of order 0 and  $x_{02}$  is its second zero. Thus the form factor integrand (12) only receives a contribution from  $J_z$ . The (un-normalized) pump fields are

$$\mathbf{E}_1 = E_0 \omega_1 \frac{x'_{01}}{a} \left( J'_0(\rho) \sin \frac{\pi z}{d} \hat{\phi} \right) \sin(\omega_1 t) \quad (\text{S2})$$

$$\mathbf{E}_2 = E_0 \frac{x_{01}^2}{a^2} J_0(\rho) \hat{\mathbf{z}} \cos(\omega_2 t) \quad (\text{S3})$$

$$\mathbf{B}_1 = E_0 \frac{(x'_{01})^2}{a^2} \left( \frac{\pi x'_{01}}{d} J'_0(\rho) \cos \frac{\pi z}{d} \hat{\rho} + J_0(\rho) \sin \frac{\pi z}{d} \hat{\mathbf{z}} \right) \cos(\omega_1 t) \quad (\text{S4})$$

$$\mathbf{B}_2 = -E_0 \omega_2 \frac{x_{01}}{a} J'_0(\rho) \hat{\phi} \sin(\omega_2 t) \quad (\text{S5})$$

where  $x_{01}$  is the first zero of  $J_0$  and  $x'_{01}$  is the first zero of  $J'_0$ . The component of  $\mathbf{J}$  with frequency  $2\omega_1 - \omega_2$  will contain two mode 1 fields and one mode 2 field, i.e. terms like  $\mathbf{E}_1^2 \mathbf{B}_2$ .

For the heavy mass case  $m_a \rightarrow \infty$ , inspecting Eq. (14) and keeping track of the time dependence, we have that the component of  $J_a$  quadratic in mode 1 and linear in mode 2 is

$$J_{\infty,z}^{(112)} = E_{1,\phi} s_1 \frac{\partial}{\partial \rho} \left( E_{1,\phi} B_{2,\phi} s_1 s_2 + E_{2,z} B_{1,z} c_1 c_2 \right) + B_{1,z} c_1 \left( E_{1,\phi} B_{2,\phi} (\omega_1 c_1 s_2 + \omega_2 s_1 c_2) - E_{2,z} B_{1,z} (\omega_1 s_1 c_2 + \omega_2 c_1 s_2) \right) \quad (\text{S6})$$

where  $s_{1,2} = \sin(\omega_{1,2} t)$  and  $c_{1,2} = \cos(\omega_{1,2} t)$ .

At this point,  $J_{\infty,z}^{(112)}$  has frequency components  $\omega_2$ ,  $2\omega_1 - \omega_2$ , and  $2\omega_1 + \omega_2$ . We now wish to isolate the frequency component at  $\omega_s = 2\omega_1 - \omega_2$ . To do this, we note that terms appear such as

$$\sin^2(\omega_1 t) \sin(\omega_2 t) = \frac{1}{2} \sin(\omega_2 t) + \frac{1}{4} \sin((2\omega_1 - \omega_2)t) - \frac{1}{4} \sin((2\omega_1 + \omega_2)t), \quad (\text{S7})$$

so to isolate the desired frequency component, we make the replacement

$$s_1^2 s_1 \rightarrow \frac{1}{4}. \quad (\text{S8})$$

Similarly, for the other two terms we have

$$s_1 c_1 c_2 \rightarrow \frac{1}{4}, \quad c_1^2 s_2 \rightarrow -\frac{1}{4}, \quad (\text{S9})$$

where in all three cases only the  $\sin(\omega_s t)$  phase component appears (i.e. there is no  $\cos(\omega_s t)$  term). Thus the component of  $J_{a,z}^{(112)}$  oscillating at the signal frequency is

$$J_{\infty,z} |_{\omega_s} = \frac{1}{4} \left\{ E_{1,\phi} \frac{\partial}{\partial \rho} \left( E_{1,\phi} B_{2,\phi} + E_{2,z} B_{1,z} \right) + B_{1,z} (\omega_2 - \omega_1) \left( E_{1,\phi} B_{2,\phi} + E_{2,z} B_{1,z} \right) \right\} \sin(\omega_s t). \quad (\text{S10})$$



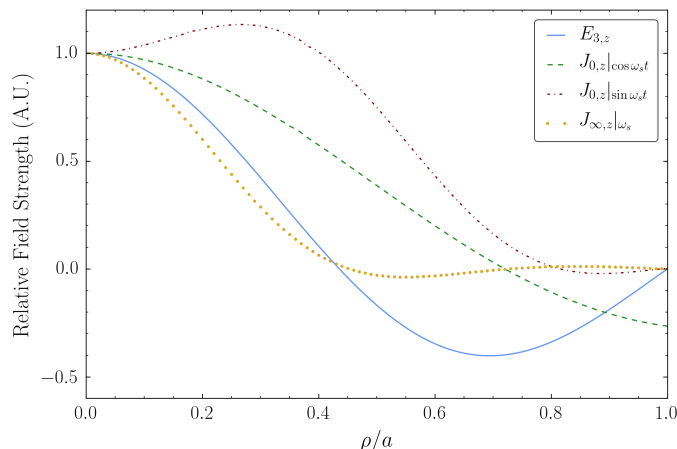


FIG. S1: Signal mode  $E_{s,z}$  and ALP-induced effective currents  $J_{\infty,z}|_{\omega_s}$  and  $J_{0,z}|_{\omega_s}$  for the TE<sub>011</sub>/TM<sub>010</sub>/TM<sub>020</sub> mode combination. There is no  $\phi$  dependence in either the signal mode or the effective currents; the mode profiles are evaluated at  $z = d/2$ , normalized to 1 at  $\rho = 0$ , and plotted as a function of the remaining variable  $\rho$ . The similar profiles to the signal mode for  $J_{\infty,z}$  and both phases of  $J_{0,z}$  leads to a large form factor for this mode choice.

Plugging (S2)–(S5) into Eq. (S10), we see that the  $z$ -dependence of all terms is  $\sin^2(\frac{\pi z}{d})$ , and there is no  $\phi$  dependence. Evaluating Eq. (S10) with  $\omega_1 = 3.96245/a$  and  $\omega_2 = 2.40483/a$  which satisfies the frequency-matching condition for the third mode at  $z = d/2$ , we obtain  $J_{\infty,z}(\rho)|_{\omega_s}$ , which is plotted in Fig. S1. For comparison, we also plot  $E_{3,z}(\rho)$  with both profiles normalized to 1 at  $\rho = 0$ , showing that the shape of these functions is fairly similar and we expect a large overlap.

As noted in the main text, the current  $\mathbf{J}_0$  in the light mass case is nonlocal, so there is no simple analytic expression in terms of the pump fields. Nonetheless, we can evaluate the spatial integrals in Eq. (12) numerically, and isolate the frequency components as described above. Unlike the heavy mass case, both phase components  $\sin(\omega_s t)$  and  $\cos(\omega_s t)$  are present. The two phase components of  $\mathbf{J}_{0,z}$  are also shown in Fig. S1; note that the component which is in phase with the pump modes vanishes at the boundary  $\rho = a$ , while the other phase component does not.

### Characteristics of light and heavy form factors

In order to test the feasibility of our proposed method, we searched through a number of cylindrical cavity mode combinations and calculated the expected coupling  $K_\infty$  for each. Since there are, in principle, infinitely many possible mode combinations, we restricted to the six smallest non-trivial mode numbers for each field and mode number. We also took advantage of three selection rules for modes TE <sub>$n$  $p$  $q$</sub>  and TM <sub>$n$  $p$  $q$</sub> :

- Either  $\pm 2n_1 \pm n_2 = n_s$  (including all sign combinations) or  $n_2 = n_s$ .
- Either  $\pm 2q_1 \pm q_2 = q_s$  (including all sign combinations) or  $q_2 = q_s$ .
- If  $\omega_2$  and  $\omega_s$  are both TE modes or both TM modes, then  $\mathbf{E}_s$  and  $\mathbf{B}_s$  must have the same  $\cos n\phi$  dependence as  $\mathbf{E}_{1,2}$  and  $\mathbf{B}_{1,2}$ , rather than  $\sin n\phi$ .

We found several modes with  $K_\infty$  in the range 0.1–0.2. We then chose five of these with generally smaller mode numbers and calculated  $K_0$  for each in order to test whether the same cavity dimensions would allow for effective searches of both high- and low-mass ALPs. As noted above, because  $K_0$  contains both phase components  $\sin(\omega_s t)$  and  $\cos(\omega_s t)$ , we compute  $K_0$  by summing the form factors in quadrature for the two phase components. As described in the main text, this is appropriate for photon counting at the standard quantum limit, but in future work we will explore the benefits of phase-sensitive amplifiers, in which case one quadrature may dominate. The values of  $K_\infty$  and  $K_0$  for each of these five modes are given in Table S1.

We conclude that a precise choice of modes is not necessary for achieving a large cavity form factor for both heavy and light ALPs, though we find that the largest form factors come from  $\omega_1 = \text{TE}_{011}$  and  $\omega_2$  and  $\omega_s$  being TM modes. These general properties are easy to reproduce in an elliptical cavity, which will likely be the basis for a realistic design.

$\omega_1$	$\omega_2$	$\omega_s$	$K_\infty$	$K_0$
TE <sub>011</sub>	TM <sub>010</sub>	TM <sub>020</sub>	0.18	0.24
TE <sub>011</sub>	TM <sub>011</sub>	TM <sub>013</sub>	0.12	0.080
TE <sub>011</sub>	TM <sub>012</sub>	TM <sub>014</sub>	0.13	0.075
TE <sub>011</sub>	TM <sub>030</sub>	TM <sub>050</sub>	0.11	0.079
TE <sub>011</sub>	TM <sub>040</sub>	TM <sub>060</sub>	0.12	0.062

TABLE S1: The values of  $K_\infty$  and  $K_0$  for five mode combinations with relatively large values of  $K_\infty$  and small mode numbers. Note that, for all five mode combinations,  $K_0$  is within a factor of 2 of  $K_\infty$ , making it reasonable to use the same cavity to search for both high- and low-mass ALPs.